



RESEARCH PAPER

Modulation of plant architecture by the miR156f–OsSPL7–OsGH3.8 pathway in rice

Zhengyan Dai^{1,*}, Jiang Wang^{2,*}, Xiaofang Yang^{1,3}, Huan Lu², Xuexia Miao¹ and Zhenying Shi^{1,†} 

¹ Key Laboratory of Insect Developmental and Evolutionary Biology, Institute of Plant Physiology and Ecology, Shanghai Institutes for Biological Sciences, Chinese Academy of Sciences, No. 300 Fenglin Road, Shanghai, China

² National Key Laboratory of Plant Molecular Genetics, Institute of Plant Physiology and Ecology, Shanghai Institutes for Biological Sciences, the Chinese Academy of Sciences, No. 300 Fenglin Road, Shanghai, China

³ University of the Chinese Academy of Sciences

*These authors contributed equally to this work

† Correspondence: zyshi@sibs.ac.cn

Received 9 January 2018; Editorial decision 10 July 2018; Accepted 16 July 2018

Editor: Zoe Wilson, University of Nottingham, UK

Abstract

Tiller number and plant height are two of the main features of plant architecture that directly influence rice yield. Auxin and miR156, an extensively studied small RNA (smRNA), are both broadly involved in plant development and physiology, suggesting a possible relationship between the two. In this study, we identified a rice T-DNA insertion cluster and dwarf (*cd*) mutant that has an increased tiller number and reduced plant height. The T-DNA insertion was in close proximity to the *miR156f* gene and was associated with its up-regulation. Plants overexpressing *miR156f* resembled the *cd* mutant. In contrast, plants overexpressing an *miR156f* target mimic (MIM156fOE) had a reduced tiller number and increased height. Genetic analysis showed that *OsSPL7* is a target of *miR156f* that regulates plant architecture. Plants overexpressing *OsSPL7* had a reduced tiller number, while *OsSPL7* RNAi plants had an increased tiller number and a reduced height. We also found that *OsSPL7* binds directly to the *OsGH3.8* promoter to regulate its transcription. Overexpression of *OsGH3.8* and *OsGH3.8* RNAi partially complemented the MIM156fOE and *cd* mutant phenotypes, respectively. Our combined data show that the miR156f–OsSPL7–OsGH3.8 pathway regulates tiller number and plant height in rice, and this pathway may allow crosstalk between miR156 and auxin.

Keywords: Auxin, miR156f, *Oryza sativa*, OsGH3.8, OsSPL7, plant architecture, tiller.

Introduction

Rice (*Oryza sativa*) is a staple food for nearly half of the world's population. To address the imbalance between increasing population demands and decreasing availability of arable land, many breeding programs focus on improving grain yield and plant architecture to increase productivity. Tiller number and plant height are two important

agronomic traits that directly contribute to plant architecture (Zhang, 2007).

Auxin was the first plant hormone to be identified, and is involved in an extraordinarily broad spectrum of developmental and physiological processes (Sauer *et al.*, 2013). Examples of these include axillary bud dormancy, ectopic

Abbreviations: MIM156f, mimicry miR156f; MIM156fOE, mimicry miR156f overexpression; miR156fOE, miR156f overexpression; OsGH3.8OE, *OsGH3.8* overexpression; OsGH3.8RNAi, *OsGH3.8* RNA interference; OsGH3.8R, *OsGH3.8* RNA interference transgenic plants; SPL7Flag, *OsSPL7* fused with the Flag tag driven by its own promoter; SPL2GFP, *OsSPL2* fused with GFP driven by its own promoter; SPL7OE, *OsSPL7* overexpression; SPL2OE, *OsSPL2* overexpression; SPL13OE, *OsSPL13* overexpression; SPL7RNAi, *OsSPL7* RNA interference; smRNA, small RNA; SPL, *SQUAMOSA PROMOTER BINDING PROTEIN-like*.

© The Author(s) 2018. Published by Oxford University Press on behalf of the Society for Experimental Biology.

This is an Open Access article distributed under the terms of the Creative Commons Attribution License (<http://creativecommons.org/licenses/by/4.0/>), which permits unrestricted reuse, distribution, and reproduction in any medium, provided the original work is properly cited.

shoot development, and leaf angle (Yoshida *et al.*, 2012; Zhao *et al.*, 2013). Because of the universal role of auxin and its rapid action, auxin levels are tightly controlled by the concerted co-operation of biosynthesis, metabolism, and transport in plants. In Arabidopsis, nearly 95% of auxins exist as amino acid and protein conjugates (Ljung *et al.*, 2002; Woodward and Bartel, 2005). Some of these molecules act as intermediates for degradation, and some provide a reusable metabolite pool for free indole-3-acetic acid (IAA) (LeClere *et al.*, 2002; Rampey *et al.*, 2004). Auxin rapidly and transiently induces the accumulation of at least three families of transcripts: *SMALL AUXIN-UP RNAs* (*SAURs*), *GH3*-related transcripts, and *AUXIN/IAA* (*Aux/IAA*) family members (Woodward and Bartel, 2005). The *GH3* family of acyl-acid-amido synthetases catalyzes the ATP-dependent formation of amino acid conjugates with plant hormones, including auxins and jasmonates (Chen *et al.*, 2010). This family is present in various plant species, and includes 19 members in Arabidopsis and 13 in rice (Staswick *et al.*, 2002; Terol *et al.*, 2006; Jain and Khurana, 2009). *GH3* enzymes are grouped into three families according to their sequence homology and acyl-acid substrate preference. Two of these families are present in rice: class I and II, which mediate jasmonate and salicylic acid conjugation, respectively (Staswick *et al.*, 2002; Westfall *et al.*, 2010).

Small RNAs (smRNAs) are non-coding RNAs of ~22 nucleotides (nt) in length. There are two broad categories of smRNA, miRNAs and siRNAs (Aravin *et al.*, 2003; Bartel and Bartel, 2003; Bartel, 2004). We have witnessed an explosion in our understanding of smRNAs across different species. Improved understanding of the mechanisms by which smRNAs interact with their target RNAs and the important roles of smRNA in various developmental and physiological processes have revealed that smRNAs are simple in their core mechanism but have profound functions (Nelson *et al.*, 2003; Bartel, 2009). Moreover, the sequences, mechanisms, and functions of miRNAs are conserved across species (Jones-Rhoades, 2012).

Plant miRNAs target key developmental regulators, many of which are transcription factors (Rhoades *et al.*, 2002; Jones-Rhoades *et al.*, 2006). Among them, miR156 has a wide scope (Wang and Wang, 2015) that includes transition from vegetative to reproductive growth and flowering time (Wu *et al.*, 2009; Huijser and Schmid, 2011; Wang, 2014; S. Yu *et al.*, 2015), embryo patterning (Nordine and Bartel, 2010), gibberellin-mediated flowering (Yu *et al.*, 2012), age-dependent flowering (Bergonzi *et al.*, 2013), gynoecium differential patterning (Xing *et al.*, 2013), leaf development (Xie *et al.*, 2012), trichome distribution (Xue *et al.*, 2014), lateral root development (N. Yu *et al.*, 2015), plant architecture (Bhogale *et al.*, 2014; Chen *et al.*, 2015), biosynthesis of secondary metabolites such as anthocyanin and sesquiterpene (Gou *et al.*, 2011; Z.X. Yu *et al.*, 2015), ovary and fruit development (Ferreira e Silva *et al.*, 2014), and developmental timing (Cho *et al.*, 2012). In rice, ectopic expression of miR156b and miR156h results in dwarfism, a small panicle, and delayed flowering (Xie *et al.*, 2006). Together with miR529 and miR172, miR156 regulates vegetative and reproductive branching (Wang *et al.*, 2015). One target of miR156, *SQUAMOSA PROMOTER BINDING PROTEIN-like14*

(*SPL14*), regulates optimal plant architecture and has great potential for improving rice yield (Jiao *et al.*, 2010; Miura *et al.*, 2010; Springer, 2010). Another target, *OsSPL16*, regulates rice seed size and quality (Wang *et al.*, 2012). Furthermore, miR156 responds to various abiotic and nutritional stresses (Jia *et al.*, 2010; Zhou *et al.*, 2010; Nischal *et al.*, 2012; Wang *et al.*, 2013; Cui *et al.*, 2014; Stief *et al.*, 2014; Song *et al.*, 2015).

The functional activity and universality of both miR156 and auxin led to the hypothesis that there is crosstalk between them in regulating plant architecture. In this study, we identified a cluster and dwarf (*cd*) mutant that had underlying up-regulation of miR156f. Genetic analysis of miR156f and the *OsSPL7* gene showed that the miR156f/*OsSPL7* module regulates plant architecture, with ectopic expression of miR156f and down-regulation of *OsSPL7* leading to plants with an increased number of tillers and reduced height. Moreover, ectopic expression of an miR156f target mimic (MIM156f) and up-regulation of *OsSPL7* dramatically reduced the number of tillers. Further biochemical and genetic analyses confirmed that *OsSPL7* directly regulates transcription of the *OsGH3.8* gene and the involvement of auxin in regulating plant architecture through the miR156f/*OsSPL7* pathway. Our findings may provide a useful breeding resource for modifying rice plant architecture and enhancing rice yield.

Materials and methods

Plant species and growth conditions

The rice *cd* mutant was selected from a T-DNA insertion collection generated from the wild type (WT) Zhonghua 11 (*Oryza sativa* L. subsp. *japonica* cv. Zhonghua No. 11, ZH11) (Wang *et al.*, 2004). All the rice plants were grown in a greenhouse, with 10 h light and 14 h dark, or in the field under natural conditions in summer, Shanghai, China.

Tiller outgrowth analysis

Four-week-old rice seedlings were used for analysis; plants were peeled carefully to expose the young tiller buds in the basal region where tillers begin to develop.

Treatment of rice plants with naphthaleneacetic acid (NAA)

Four-week-old WT rice seedlings were watered with 10 μ M NAA, and samples were collected at the indicated time after treatment.

Expression profile analysis

For expression profile analysis of miR156f, and some *OsSPL* genes, 1-month-old WT plants were used to collect leaf, leaf sheath, roots, and stems; and young panicles were collected at the reproductive stage from the WT.

Anatomical analysis and in situ hybridization

Anatomical analysis and *in situ* hybridization were carried out as previously described by Wang *et al.* (2010) and Dai *et al.* (2016), respectively.

Plasmid construction and transformation of rice

The full-length *IPS* gene of Arabidopsis was amplified by KOD-plus DNA polymerase (TOYOBO) using primers IPSF and IPSR, cloned into the PBSK vector using *Bam*HI and *Kpn*I, and the mature miRNA

region was substituted into the MIM156f sequence using overlapping PCR (Higuchi *et al.*, 1988); IPSF was paired with MIM156R and IPSR with MIM156F to get the substituted sequence into two separate but overlapping PCR fragments, and then used as template. IPSF and IPSR were used as primers to amplify the full-length IPS-MIM156f fragment. The IPS-MIM156f fragment was re-cloned into p1301-35SNos vector to form the MIM156fOE vector.

OsSPL7, *OsSPL2*, *OsSPL13*, and *OsGH3.8* overexpression (OE) vectors were constructed by cloning full-length cDNA of respective genes into the p1301-35SNos vector using *Bam*HI and *Kpn*I double digestion.

RNAi of *OsSPL7* (SPL7RNAi) and *OsGH3.8* (GH3.8R) were constructed by cloning a 466 bp and a 273 bp cDNA fragment, respectively, into p1301RNAi vector in the sense orientation using *Bam*HI and *Kpn*I, and in the antisense orientation using *Sac*I and *Spe*I.

OsSPL7::SPL7Flag (SPL7Flag) vector was constructed by cloning the full-length cDNA of *OsSPL7* in-frame into the p1305 vector using *Kpn*I and *Bam*HI, and the *OsSPL7* promoter was further cloned using *Sac*I and *Kpn*I.

SPL7::GUS plasmid was constructed by amplifying the *OsSPL7* promoter using primers SPL7PF2 and SPL7PR and cloned into the promoter::GUS plasmid derived from pCAMBIA1301.

MIM156fOE, SPL2OE, SPL7OE, SPL13OE, SPL7RNAi, GH3.8R, SPL7::GUS, and *OsSPL7::SPL7Flag* plasmid were transformed into WT rice using the *Agrobacterium*-mediated method with minor modification (Hiei *et al.*, 1994).

RT-PCR analysis and quantitative real-time RT-PCR (qRT-PCR)

Total RNA was extracted from different tissues using TRIzol (Invitrogen), followed by DNase I digestion. For reverse transcription-PCR (RT-PCR) analysis, 1 µg of total RNA was reverse transcribed using oligo(dT) primer and M-MLV reverse transcriptase (TOYOBO) according to the manufacturer's instructions. RT-PCR analyses were performed at least three times with the *actin* gene as internal control.

For quantitative real-time PCR (qRT-PCR), cDNA was synthesized from 1 µg of total RNA using the One Step SYBR PrimeScript RT-PCR Kit (TaKaRa), and 1 µl of cDNA was used as template for real-time analysis. Sampling and expression measurement were repeated three times with the *actin* gene as internal reference.

Yeast-one-hybrid assays

The full-length cDNAs of *OsSPL2*, *OsSPL7*, and *OsSPL13* were amplified with gene-specific primers (see Supplementary Table S1 at JXB online), and then fused into the activation domain (AD) in vector pPC86. Fragments containing 'GTAC' in the *OsGH3.8* promoter were amplified with gene-specific primers and fused into the vector p178 at the *Xho*I site. The p178 and pPC86 constructs were co-transformed into the yeast strain EGY48. The yeast was grown on SD selective medium (SD-His-Leu) and observed in blue on Chromogenic medium. The transformants containing void plasmid pPC86 and p178 constructs were used as negative control. Yeast one-hybrid assay was carried out as described (Matchmaker One-hybrid System; Clontech).

miRNA northern blot analysis

Approximately 30 µg of total RNA was separated on 15% polyacrylamide denaturing gels. RNAs were transferred to Amersham Hybond™-N⁺ membranes and cross-linked by UV irradiation; the membranes were hybridized with biotin-labeled DNA probes complementary to the miRNA sequences at 42 °C overnight. The membranes were then washed and incubated with stabilized streptavidin-horseradish peroxidase at 42 °C. After washing with substrate equilibration buffer and adding stable peroxide solution and enhancer solution, the membranes were imaged using an FLA-5000 Phosphorimager. The DNA probes were synthesized and biotin labeled using a 3' end DNA labeling method.

ChIP analysis

Immunoprecipitation of DNA associated with modified histones was carried out according to the instructions of the EpiQuik™ Plant ChIP Kit. Rice young panicles were cross-linked, and Flag antibody was used for

ChIP, with normal mouse IgG as the negative control. The immunoprecipitated sample and whole-cell extract (input) were incubated at 65 °C to reverse cross-linked DNA, and ethanol precipitation to elute purified DNA. ChIP DNA and whole-cell extract (input) were subjected to 35 cycles of qRT-PCR with the primers designed to amplify a sequence in the promoter, with a sequence in the coding region as the control.

Dual luciferase (LUC) analysis

The plasmid pHB::SPL7-GFP was transformed into *Agrobacterium tumefaciens* strain GV3101 to act as an effector. The reporter construct was constructed by inserting the *OsGH3.8* promoter into the pGreenII 0800-LUC vector (Hellens *et al.*, 2005) and subsequently co-transformed with the helper plasmid pSoup19 into GV3101 to act as the reporter. pHB::GFP plasmid was used as negative control. Overnight *A. tumefaciens* cultures were collected by centrifugation, re-suspended in Murashige and Skoog (MS) medium to OD₆₀₀=0.6, and incubated at room temperature for 3 h. The reporter strain was mixed with the effectors strain harboring pHB::SPL7-GFP or pHB::GFP at a ratio of 1:1. The mixture of *A. tumefaciens* suspension was infiltrated into tobacco (*Nicotiana benthamiana*) leaves, with the experimental group and the control group infiltrated into the opposite position on the same leaves. The leaves were collected after 3 d under long-day white light conditions and infiltrated with 150 µg ml⁻¹ luciferin solution; images were captured using a CCD camera 5 min later, and quantification was performed using a Dual-Luciferase Reporter Assay System according to the instructions (Promega, Madison, WI, USA). Three biological repeats were measured for each sample.

Histochemical GUS staining

β-Glucuronidase (GUS) staining was carried out by staining different tissues of the SPL7::GUS transgenic plants in GUS reaction solution which contained 100 mM sodium phosphate, 10 mM EDTA, 0.1% (v/v) Triton X-100, and 1 mM 5-bromo-4-chloro-3-indolyl-β-glucuronic acid (Sigma, USA) with pH 7.0, overnight at 37 °C, and then clearing in 75% ethanol.

Microarray analysis

Seedlings of the 4-month old *cd* mutant and WT were used for microarray analysis. Ten plants for each sample were collected to extract total RNA and sent to the Beijing Genomics Institute for the following tests and analysis. RNA quality was checked using a NanoPhotometer[®] spectrophotometer (IMPLEN, CA, USA). A 3 µg aliquot of total RNA per sample was used as input material for the RNA library construction with NEBNext[®] Multiplex RNA Library Prep Set for Illumina[®] (NEB, USA) following the manufacturer's recommendations. After cluster generation, the library preparations were sequenced on an Illumina HiSeq2000 Platform and the clean reads were mapped to the *O. sativa* genome (RGAP, version 7.0) using cufflink software after filtering the dirty raw reads.

Subcellular localization of OsSPL7 protein in rice protoplasts

The pA7-EGFP vector was used to construct green fluorescent protein (GFP) fusion proteins or as a negative control. The coding sequence of *OsSPL7* was cloned into pA7-EGFP to generate *OsSPL7-GFP*. The mCherry-VirD2NLS (mCherry) vector was used as nuclear control. The fusion constructs or control plasmids were transformed into rice protoplasts. Fluorescence was visualized under a Zeiss Axioimager Z2 fluorescence microscope. Experiments were biologically repeated three times.

Accession numbers

OsSPL2 (LOC_Os01g69830), *OsSPL3* (LOC_Os02g04680), *OsSPL4* (LOC_Os02g07780), *OsSPL7* (LOC_Os04g46580), *OsSPL11* (LOC_Os06g45310), *OsSPL12* (LOC_Os06g49010), *OsSPL13* (LOC_Os07g32170), *OsSPL14* (LOC_Os08g39890), *OsSPL16* (LOC_Os08g41940), *OsSPL17* (LOC_Os09g31438), *OsSPL18* (LOC_Os09g32944), *OsSPL19* (LOC_Os11g30370), *OsGH3.1* (AK063368),

OsGH3.2 (LOC-Os01g55940), *OsGH3.3* (AK072125), *OsGH3.4* (AK101932), *OsGH3.5* (AK071721), *OsGH3.6* (AK106538), *OsGH3.7* (AK099376), *OsGH3.8* (AK101193), *OsGH3.9* (AK106839), *OsGH3.10* (LOC-Os07g38860), *OsGH3.11* (LOC-Os07g47490), *OsGH3.12* (LOC-Os11g08340), *OsGH3.13* (LOC-Os11g32510), *OsGH3.14* (LOC-Os11g32520).

Results

A T-DNA insertion mutant with a cluster and dwarf phenotype is associated with overexpression of miR156f

We identified a T-DNA insertion mutant from our mutant population that showed an obvious cluster (increased number of tillers) and a dwarf (decreased plant height) phenotype (Wang *et al.*, 2004), and named it *cd* (*cd* is shown in Fig. 1A and compared with the WT in Fig. 1B). Under natural field conditions in summer in Shanghai, the *cd* mutant had an average plant height of 62.7 cm, in comparison with the WT plants which were on average 94.9 cm tall. The *cd* mutant had an average of 42.1 effective tillers, while the WT plants had 14.1 (Fig. 1C). The *cd* mutant also flowered ~5–6 d later than the WT plants (data not shown).

We next carried out genetic analysis by making genetic reciprocal crosses of the *cd* mutant with the WT. The F₁ plants from both the reciprocal cross and backcross had semi-cluster and semi-dwarf phenotypes (Fig. 1C). This suggests that the phenotype of the *cd* mutant is semi-dominant. Among the 691 F₂ population of the *cd*/ZH11 cross, there were 170 taller plants, 352 average height plants, and 169 dwarf plants. The average height plants and dwarf plants were resistant to hygromycin. Among the F₂ population of the ZH11/*cd* cross, the ratio of taller to average height to dwarf plants was 211:392:189. Therefore, the

segregation ratios of both the reciprocal cross and the backcross were ~1:2:1, which is in accordance with Mendelian segregation. Furthermore, in the F₂ population, both the cluster and dwarf phenotypes showed tight co-segregation with the T-DNA insert (Supplementary Table S2). From our results, we concluded that the cluster and dwarf phenotype in the *cd* mutant was controlled by a single semi-dominant genetic locus.

Next, we isolated the T-DNA flanking sequence in the *cd* mutant using thermal asymmetric interlaced PCR (TAIL-PCR) (Liu *et al.*, 1995). This revealed that the T-DNA was integrated at position 21575719 of NC-008401.2 (<http://www.ncbi.nlm.nih.gov/>, accessed 27 July 2018), and that the *miR156f* gene is positioned ~9 kb upstream of the insertion. miRNA northern blot analysis showed that miR156f was markedly up-regulated in the *cd* mutant (Fig. 1D).

To test whether up-regulation of miR156f caused the cluster and dwarf phenotype, we cloned the *miR156f* gene and genetically overexpressed it. More than 90% of the transgenic plants (*miR156f*OE) had a cluster and dwarf phenotype that was similar to that of the *cd* mutant (Fig. 1E). We sampled five T₀ plants and confirmed miR156f overexpression in all of them (Fig. 1F). Together, these results confirm that the T-DNA insertion in the *cd* mutant causes up-regulation of miR156f, which leads to the cluster and dwarf phenotype.

Plants overexpressing an miR156f target mimic (MIM156fOE) have fewer tillers and increased plant height

To better understand the function of miR156f in rice, we constructed a target mimic of miR156f (MIM156f) and genetically overexpressed it in WT plants (Franco-Zorrilla *et al.*, 2007).

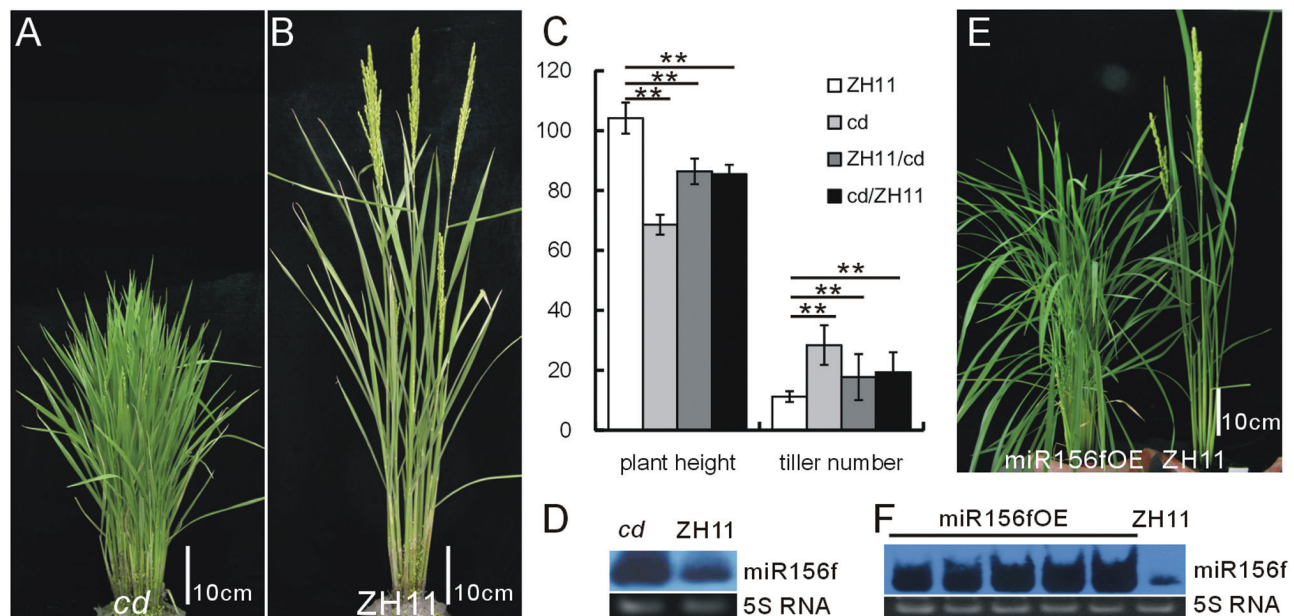


Fig. 1. Characterization of the *cd* mutant phenotype and association of miR156f expression with the cluster and dwarf phenotype. (A and B) Representative *cd* mutant (A) and WT (B) plants. (C) Plant heights and tiller numbers of the *cd* mutant, and the crosses between the *cd* mutant and WT. The asterisks represent a significant difference, as determined by a Student's *t*-test at **P*<0.05 and ***P*<0.01, respectively (*n*=20). (D) miR156f expression in the *cd* mutant. (E) Phenotype of the miR156fOE transgenic plants (left) as compared with the WT (right). (F) miR156f expression in the miR156fOE lines. (This figure is available in color at JXB online.)

Approximately 91.2% of the transgenic plants (MIM156fOE) had a reduced number of tillers and an increased plant height (Fig. 2A). MIM156f overexpression was confirmed in the transgenic plants, while endogenous miR156f was down-regulated (Supplementary Fig. S1A). Expression of *OsSPL13*, a candidate target of miR156f, was up-regulated (Supplementary Fig. S1A). These results suggest that MIM156f expression interferes with the expression of endogenous miR156f and its targets.

The T₁ generation of MIM156fOE plants were grown in the field and analyzed. The MIM156fOE plants had an average of 5.1 tillers, in comparison with 14.1 tillers in the WT plants. The MIM156fOE plants had an average height of 102.5 cm, while the average height of the WT plants was 94.9 cm (Fig. 2B). Further analysis revealed that miR156f expression influenced the elongation of the internodes in rice plants. The length of almost every internode was increased in the MIM156fOE plants, while it was reduced in the *cd* mutant. These changes in internode length influenced the overall plant height accordingly (Fig. 2C, D).

Development of tillers in rice involves two successive processes: the formation of an axillary bud at the basal region of the stem, and subsequent outgrowth. A defect in either process can influence the number of tillers (Li *et al.*, 2003). We examined the role of miR156f at the tiller initiation stage, and found that there were fewer axillary buds at the basal region of the stem in young MIM156fOE plants, in comparison with the WT (Fig. 2E). In contrast, there were more axillary buds in the *cd* mutant in comparison with the WT (Fig. 2E). These data suggest that miR156f regulates the initiation of the axillary buds. Our combined data show that miR156f regulates tiller number and plant height in rice.

Transgenic plants overexpressing OsSPL7 have a single tiller and OsSPL7 RNAi plants have a cluster and dwarf phenotype

miRNAs function mainly through negative regulation on their targets. In rice, there are 12 and 18 genes coding for miR156f and its target *OsSPL* genes, respectively (<http://www.mirbase.org>, accessed 27 July 2018; Xie *et al.*, 2006). In the microarray analysis of the *cd* mutant, most of the *OsSPL* genes were down-regulated. Among these genes, *OsSPL2*, *OsSPL7*, and *OsSPL13* were the most down-regulated, according to the fold change (Supplementary Table S3). We examined *OsSPL* expression in the *cd* mutant, miR156fOE, and MIM156fOE plants using qRT-PCR, and further confirmed the regulatory effect of miR156f on the expression of most *OsSPL* genes (Supplementary Fig. S1B). To examine miR156f function further, we carried out genetic analysis of *OsSPL2*, *OsSPL7*, and *OsSPL13*.

First, we individually overexpressed each of these three genes in the WT background. Transgenic plants overexpressing *OsSPL7* (SPL7OE) had thickened roots with fewer lateral roots (Fig. 3B), and resembled the MIM156fOE phenotype (Fig. 3A). Cellular analysis revealed that the thickened roots in the MIM156fOE plants were associated with an increased number of parenchymal cells (Supplementary Fig. S2A–C). Furthermore, most SPL7OE plants had single tillers and were short and infertile (Fig. 3C). To rule out the possibility that the infertility of the SPL7OE plants might be caused by high-level expression of *OsSPL7* under the 35S promoter, we generated SPL7Flag transgenic lines with *OsSPL7* under its native promoter and fused to a Flag tag. In these SPL7Flag plants, the *OsSPL7* gene was still up-regulated, but to a lesser degree than in the SPL7OE plants (Fig. 3D). Moreover, the

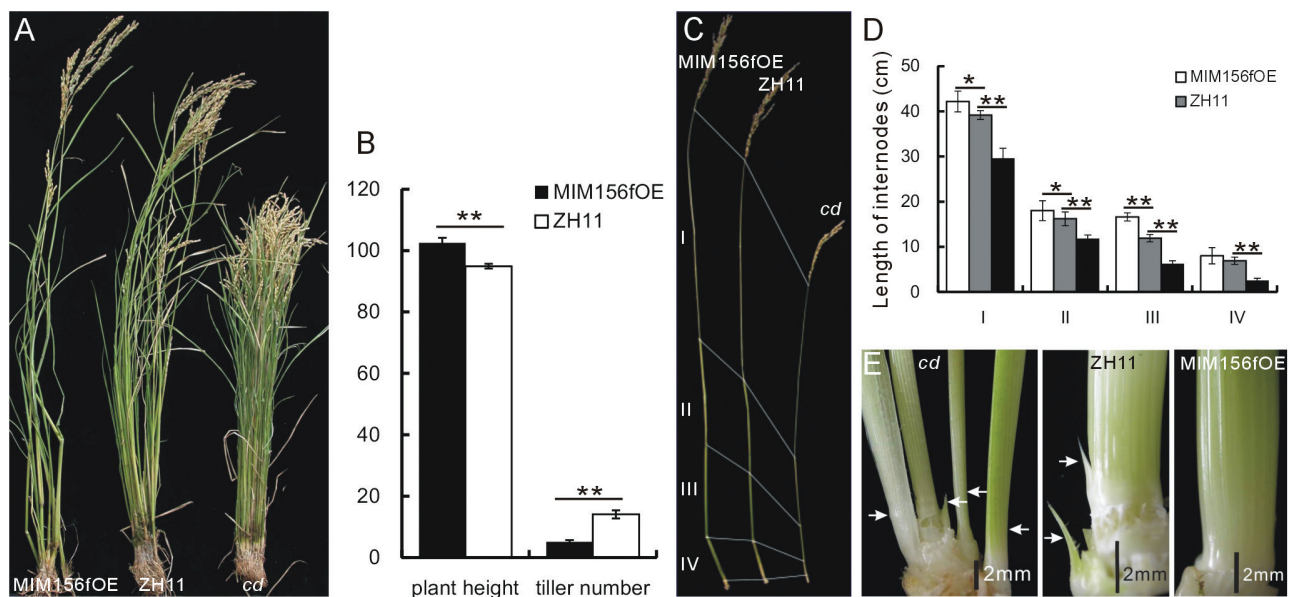


Fig. 2. Phenotype of the MIM156f OE plants. (A) The appearances of the MIM156fOE, WT, and *cd* mutant plants (left to right). (B) The plant heights and tiller numbers of the MIM156fOE plants in comparison with the WT plants ($n=20$). (C) Appearance of the stems of the MIM156fOE, WT, and *cd* mutant plants, showing the numbered internodes I, II, III, IV. (D) Lengths of each internode in the MIM156fOE, WT, and *cd* mutant plants ($n=10$). The asterisks in (B) and (D) represent a significant difference, as determined by a Student's *t*-test at $*P<0.05$ and $**P<0.01$, respectively. (E) The basal region of the stems of the *cd* mutant, WT, and MIM156fOE plants (left to right). (This figure is available in color at JXB online.)

phenotype of the SPL7Flag plants was not as severe as that of the SPL7OE plants. The SPL7Flag plants had a reduced height in comparison with the WT (Fig. 3E, F), but a similar tiller number. We also constructed *OsSPL7* RNAi transgenic plants (SPL7RNAi), which had reduced plant heights and increased tiller numbers, and resembled the *cd* mutant and the miR-156fOE plants (Fig. 3E, F).

To characterize *OsSPL7* further, we analyzed its expression profile together with that of miR156f (Fig. 4A). miR156f was expressed at low levels in the roots and very young panicles (2 cm in length). However, there was clear *OsSPL7* expression in the root (Fig. 4B), in accordance with its function in root development (Fig. 3B). In young panicles, *OsSPL7* showed a relatively high expression level (Fig. 4B). In comparison, expression of *OsSPL2* and *OsSPL13* was not as high in the roots, and, similarly, both *OsSPL2* and *OsSPL13* showed high expression in the 2 cm panicle whereas miR156f was undetectable (Fig. 4B). We also constructed SPL7::GUS transgenic plants in which the *OsSPL7* promoter was used to drive *GUS* gene expression. The *GUS* signal was detected in the leaf and leaf sheath (Fig. 4C, D), and the young 1.5 cm panicle (Fig. 4F), but not the leaf ligule or the leaf auricle (Fig. 4E). *In situ* hybridization confirmed the *OsSPL7* expression at the early stage of panicle development (Fig. 4G). Together, these results suggest that *OsSPL7* is a ubiquitous protein.

We also examined *OsSPL7*-GFP fusion protein expression in rice protoplasts and found that the fluorescence signal was exclusively concentrated in the nucleus (Fig. 4I).

Plants overexpressing *OsSPL13* (SPL13OE) had a similar phenotype to that of SPL7Flag plants, while plants overexpressing *OsSPL2* alone (SPL2OE) or tagged with GFP (SPL2GFP) both had reduced plant height and increased tiller numbers, and resembled the *cd* mutant (Fig. 3E, F).

These genetic analyses suggest that several *OsSPL* genes might be involved in the regulation of plant architecture, but with differing degrees of activity and function. In this study, we chose to focus on *OsSPL7* as the downstream target of miR156f due to its phenotypic similarity to miR156f genetic plants.

We also found that there was up-regulation of miR156f in SPL2OE, SPL7OE, and SPL13OE plants, indicating that increased *OsSPL* expression has feedback regulation effects on miR156f (Supplementary Fig. S1C).

OsGH3.8 is directly regulated by *OsSPL7*

The role of auxin in maintaining apical dominance by suppressing axillary development is important. The *cd* mutant developed more ectopic shoots, while there were fewer in the MIM156fOE plants. Moreover, in the *cd* mutant, the dormancy of axillary buds was disrupted, especially in the upper nodes (Supplementary Fig. S2D). The disturbed axillary bud dormancy and ectopic shoots in the *cd* mutant suggested the possible involvement of auxin in miR156f function. To investigate this, we examined the *cd* mutant microarray data for auxin factors and found that *OsGH3.8* was up-regulated among the *OsGH3* family genes (Supplementary Table S3). Further, qRT-PCR analysis confirmed that *OsGH3.8* was the

most significantly up-regulated of these genes in the *cd* mutant (Supplementary Fig. S1D).

We further measured *OsGH3.8* expression in the *cd* mutant, the WT, and MIM156fOE plants, and found that *OsGH3.8* was up-regulated in the *cd* mutant and down-regulated in MIM156fOE plants (Fig. 5A; Supplementary Fig. S3A). Moreover, *OsGH3.8* was down-regulated in SPL7Flag plants and up-regulated in SPL7RNAi plants (Fig. 5B; Supplementary Fig. S3B). These data suggest that miR156f/*OsSPL7* might modulate plant architecture by regulating *OsGH3.8*.

Next, we examined whether there were any SPL-binding motifs in the 2 kb *OsGH3.8* promoter (<http://www.dna.affrc.go.jp/PLACE/signalscan.html>). We identified three GTAC motifs, located 1022, 1932, and 1936 bp upstream of the ATG initiation codon (Fig. 5C). Using a yeast one-hybrid approach, we found that *OsSPL7* could bind to the 1022 bp motif. When the GTAC motif was mutated to GAAC, *OsSPL7* could no longer bind to it (Fig. 5D), indicating that *OsSPL7* specifically binds to the *OsGH3.8* promoter through the GTAC motif. Moreover, our yeast one-hybrid analysis also showed that *OsSPL2* and *OsSPL13* could bind to the 1022 bp GTAC motif (Fig. 5D). These data suggest that at least some SPL proteins can bind to the *OsGH3.8* promoter.

ChIP analysis of the SPL7Flag plants using a Flag antibody showed obvious binding to the sites corresponding to the 1022 bp motif (site1; Fig. 5E) and the combined 1932 bp and 2426 bp motifs (site2; Fig. 5E). Furthermore, to validate the activation of the *OsGH3.8* gene by *OsSPL7*, we carried out a dual-LUC assay in tobacco leaf; it was revealed that *OsSPL7* activated the expression of the *OsGH3.8* gene promoter which showed a higher value of LUC/REN than the GFP control (Fig. 5F, G).

From our combined analyses, we conclude that *OsSPL7* can directly bind to the *OsGH3.8* promoter and regulate its expression.

Overexpression of *OsGH3.8* partially complements the MIM156fOE phenotype

To characterize further the genetic relationship between *OsGH3.8* and miR156f, we cloned the *OsGH3.8* gene and overexpressed it in the WT background. The transgenic plants (*OsGH3.8*OE) showed up-regulation of *OsGH3.8*, an increased number of tillers, and a reduced plant height in comparison with the WT (Fig. 6A).

We next crossed the *OsGH3.8*OE-3 and *OsGH3.8*OE-4 transgenic plant lines with homozygous MIM156fOE plants. We obtained a single MIM156f/*GH3.8*OE-3 hybrid plant and two MIM156f/*GH3.8*OE-4 hybrid plants. We molecularly confirmed these genotypes by the existence of the plasmids used for transformation (Supplementary Fig. S3C). The hybrid plants had an increased number of tillers and a reduced plant height, in comparison with MIM156fOE, with phenotypes intermediate between those of MIM156fOE and *cd* mutant plants (Fig. 6A, B). *OsGH3.8* was also up-regulated in the hybrid plants (Fig. 6C).

Next, we constructed *OsGH3.8*RNAi transgenic plants (*OsGH3.8*R). Although they did not show obvious phenotypic

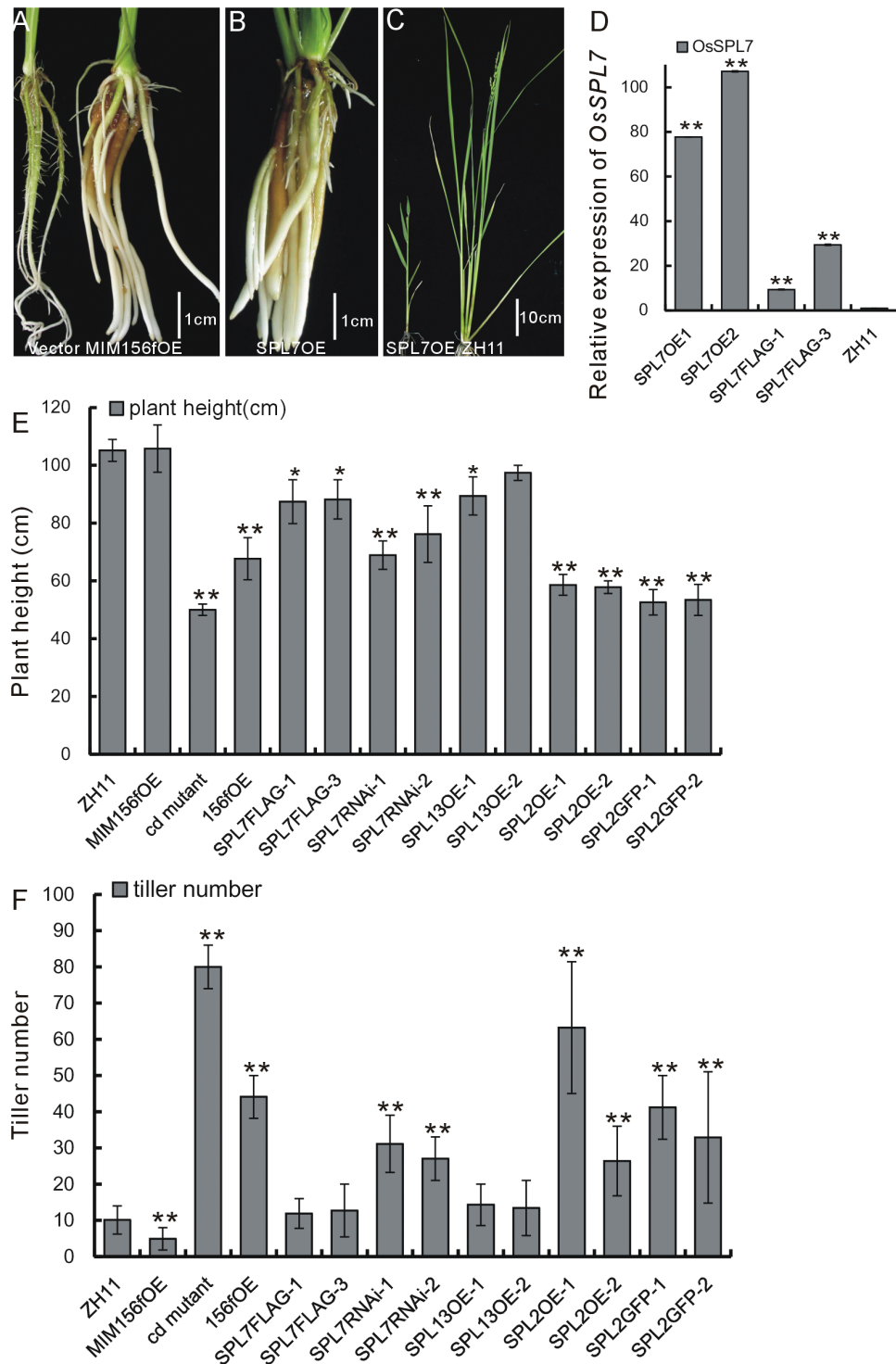


Fig. 3. Expression of *OsSPL* genes and functional activity. (A) Root phenotype of a representative T_0 generation MIM156fOE plant in a tissue culture tube (control phenotype of the transgenic plant from the empty vector is shown on the left for comparison). (B) Root phenotype of a representative T_0 generation SPL7OE plant in a tissue culture tube. (C) Appearance of a representative SPL7OE plant in comparison with a WT plant. (D) Relative expression levels of *OsSPL7* in SPL7OE and SPL7Flag plants ($n=3$). (E) Heights of the miR156- and *OsSPL*-related mutant and transgenic plants ($n=20$). (F) Tiller numbers of the miR156- and *OsSPL*-related mutant and transgenic plants ($n=20$). The asterisks in (D–F) represent a significant difference, as determined by a Student's *t*-test at * $P<0.05$ and ** $P<0.01$, respectively. (This figure is available in color at *JXB* online.)

changes in tiller number or plant height (Fig. 6D), when we crossed the *OsGH3.8R* plants with the *cd* mutant, the hybrid had obvious changes in both features that were intermediate between those of the WT and the *cd* mutant (Fig. 6D, E).

From these hybridizations, we found that *OsGH3.8* overexpression complemented the architectural defects of MIM156fOE plants by increasing the tiller number and reducing the plant height; whereas RNAi of *OsGH3.8* in the *cd*

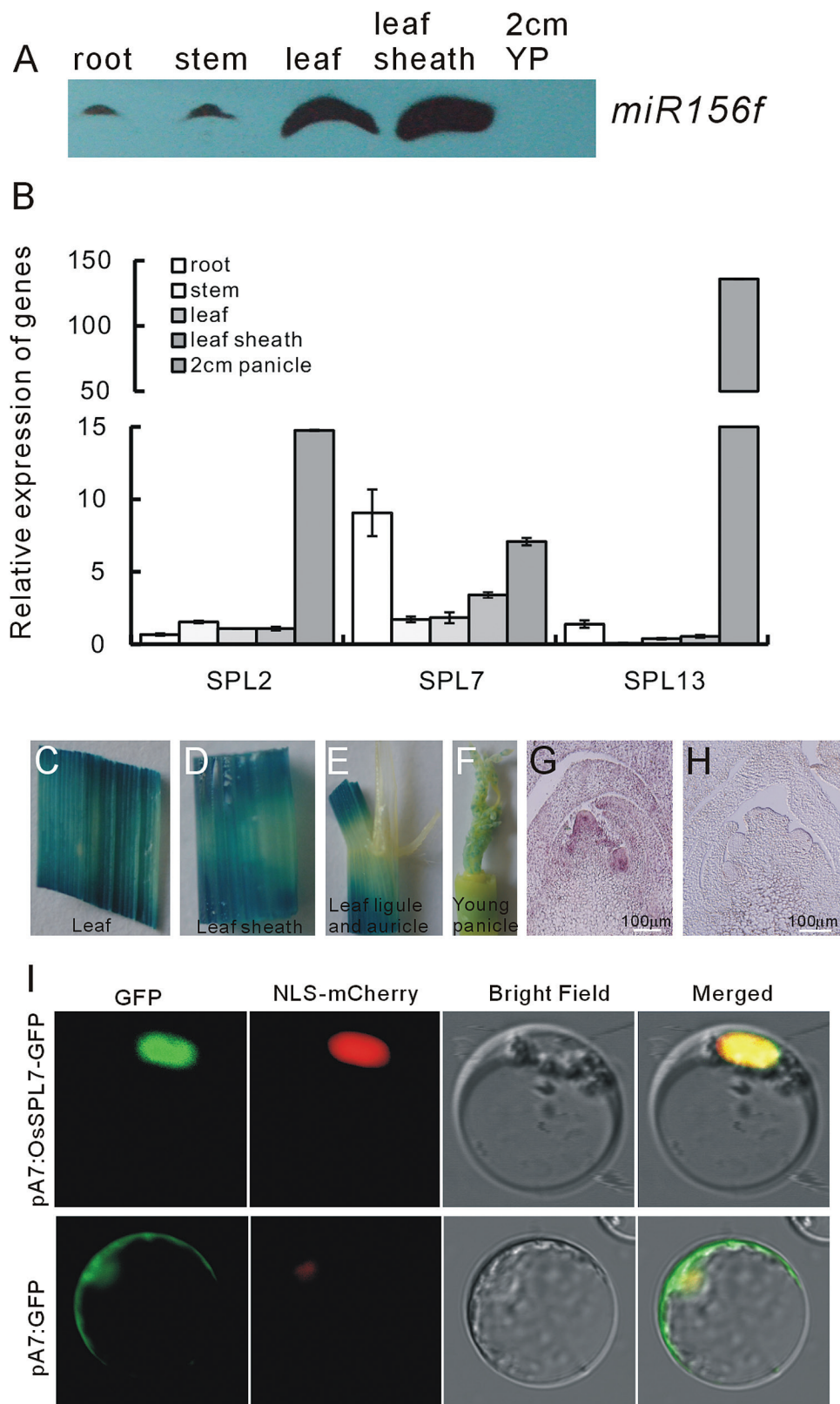


Fig. 4. miR156f and *OsSPL7* expression profiles and localization of the *OsSPL7*-GFP fusion protein. (A) Northern blot analysis of miR156f in different tissues (30 μ g of total RNA loaded for each). YP, young panicle. (B) Expression of *OsSPL2*, *OsSPL7*, and *OsSPL13* in different tissues (the same samples as in A) as revealed by qRT-PCR ($n=3$). (C-F) GUS staining of the *SPL7::GUS* transgenic plant tissues, namely the leaf (C), the leaf sheath (D), the leaf ligule and auricle (E), and the 1.5 cm panicle (F). (G) *In situ* hybridization of *OsSPL7* mRNA at the panicle initiation stage. (H) Sense probe signal from the *in situ* hybridization. (I) Localization of the *OsSPL7*-GFP fusion protein in the rice protoplast. (This figure is available in color at JXB online.)

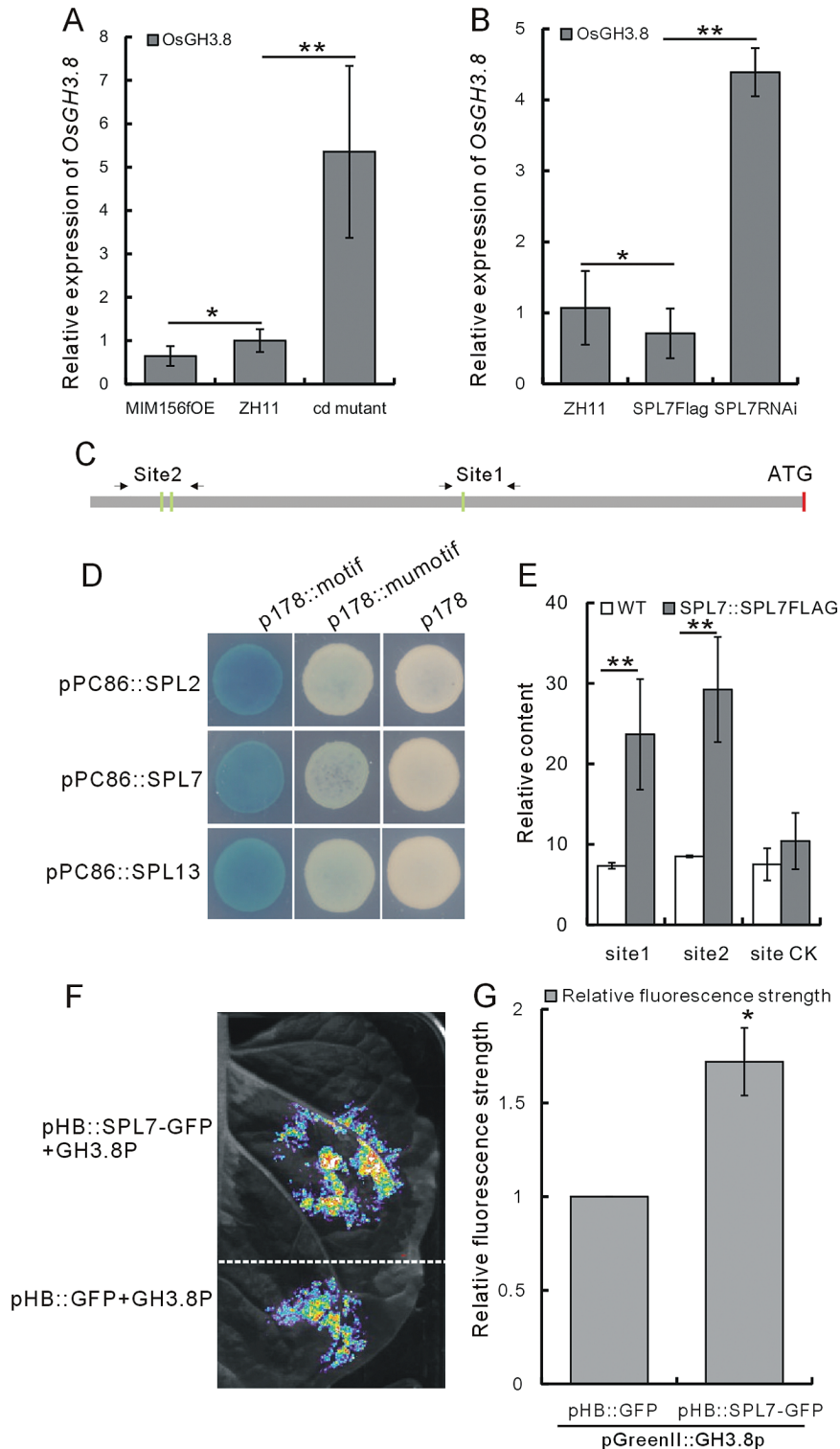


Fig. 5. Confirmation of the transcriptional regulation of the *OsGH3.8* gene by *OsSPL7* protein. (A) *OsGH3.8* expression in the *cd* mutant and the MIM156fOE plants ($n=3$). (B) *OsGH3.8* expression in the SPL7Flag and SPL7RNAi plants ($n=3$). (C) Schematic of the SPL-binding motifs in the 2 kb *OsGH3.8* promoter. Green bars indicate the positions of the GTAC motifs at 1022 bp (site 1), 1932 bp, and 1936 bp motifs (site 2). The regions amplified by the correspondingly named primers (see the Materials and methods) at sites 1 and 2 are indicated by arrows. (D) Yeast one-hybrid analysis of the *OsSPL2*, *OsSPL7*, and *OsSPL13* proteins binding to the 1022 bp motif. (E) ChIP analysis of SPL7Flag binding to sites 1 and 2 ($n=3$). (F) Image of the dual-LUC assay. (G) The LUC/REN ratio in the dual-LUC assay indicating relative luciferase activity. The empty vector pHB::GFP was used as control. Values are given as the mean \pm SD ($n=3$). The asterisks in (A), (B), (E), and (G) represent a significant difference, as determined by a Student's *t*-test at $*P<0.05$ and $**P<0.01$, respectively. (This figure is available in color at *JXB* online.)

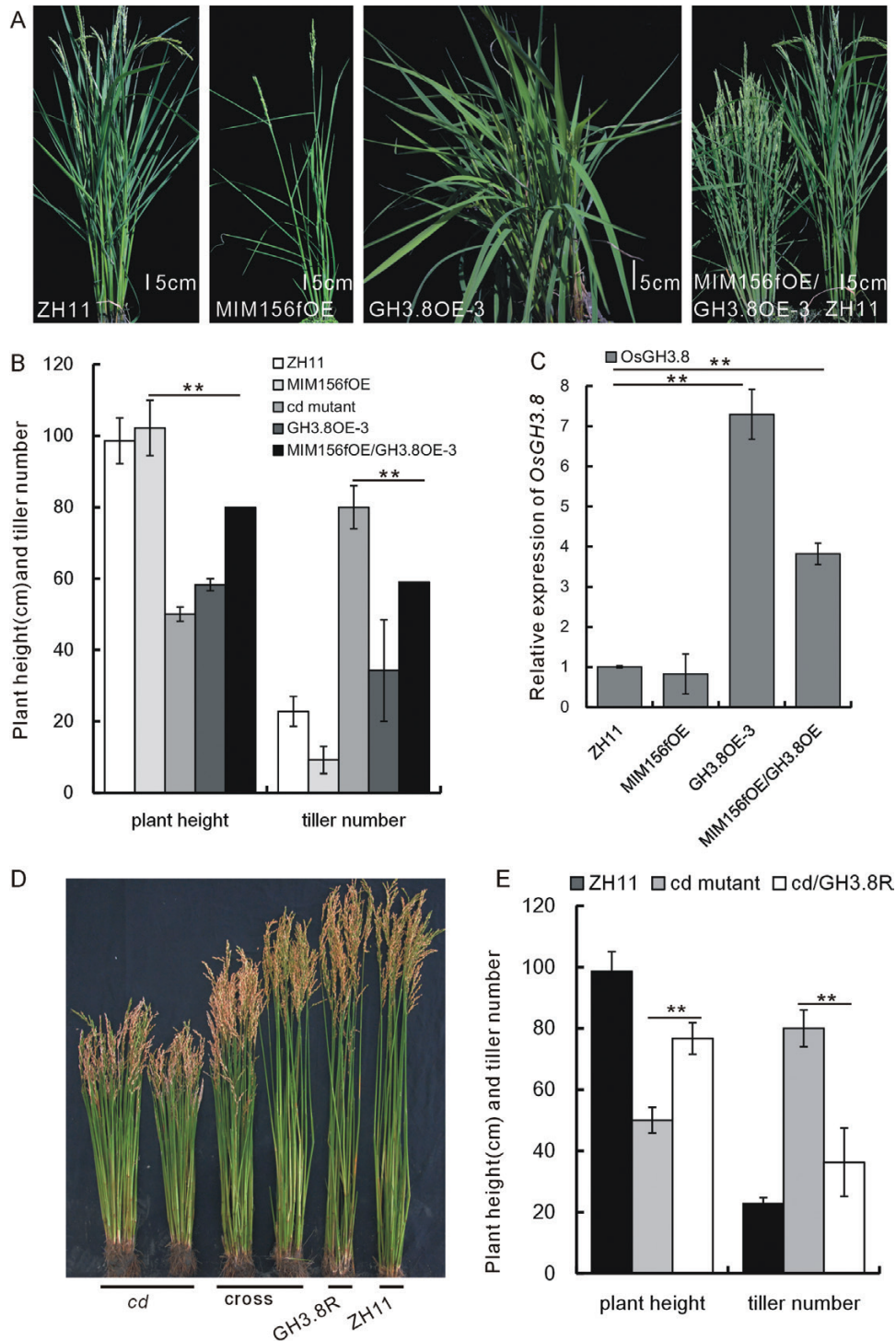


Fig. 6. Characterization of MIM156fOE/GH3.8OE and *cd*/GH3.8R hybrid plants. (A) Appearance of representative WT, MIM156fOE, GH3.8OE-3, and hybrid MIM156fOE/GH3.8OE-3 plants (left to right). (B) Plant height and tiller number of the MIM156fOE/GH3.8OE-3 hybrid and genetically related plants ($n=20$). (C) *OsGH3.8* expression in the MIM156fOE/GH3.8OE-3 plant and its parent lines ($n=3$). (D) Plant height and tiller number phenotypes of the *cd* mutant, the *cd*/GH3.8R hybrid, and the GH3.8R and WT plants (left to right). (E) Plant height and tiller number of the *cd*/GH3.8R hybrid as compared with the *cd* mutant and WT ($n=10$). The asterisks in (B), (C), and (E) represent a significant difference, as determined by a Student's *t*-test at $*P<0.05$ and $**P<0.01$, respectively. (This figure is available in color at JXB online.)

mutant complemented the *cd* mutant phenotype. The direct binding of OsSPL7 to the *OsGH3.8* promoter and the genetic relationship between miR156f and *OsGH3.8* suggest that miR156f/*OsSPL7* could directly regulate *OsGH3.8* to modulate plant architecture.

Together, we propose the following model (Fig. 7). First, miR156f negatively regulates its target *OsSPL7*, which turns out to be a negative regulator of *OsGH3.8*. *OsGH3.8* promotes the combination of IAA with aspartic acid, and the consequent change in IAA content influences plant architecture to

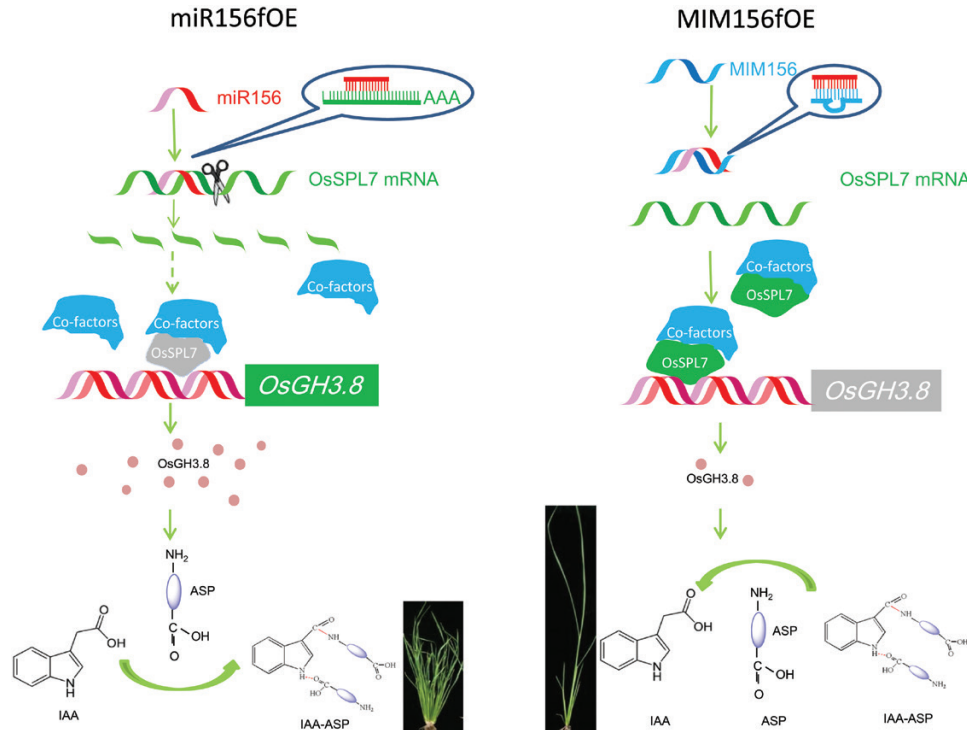


Fig. 7. Schematic of the proposed miR156–OsSPL7–OsGH3.8 pathway. In miR156fOE plants (left), excessive miR156 cleaves *OsSPL7* transcripts and represses its expression. This releases *OsSPL7* transcriptional control of *OsGH3.8* expression. The plentiful *OsGH3.8* facilitates the combination of IAA with aspartic acid (ASP), leading to cluster and dwarf plant phenotypes. In MIM156fOE plants, miR156f is sequestered by MIM156f, so that there is enough *OsSPL7* available to suppress the expression of *OsGH3.8*. This then promotes the dissociation of ASP from IAA, leading to a phenotype of reduced tiller number and increased plant height. (This figure is available in color at *JXB* online.)

alter the plant height and tiller number in rice. Since *OsGH3.8* is a fast-acting auxin-responsive gene, treatment of rice plants with NAA could rapidly induce the expression of *OsGH3.8*. This might have a feedback effect to reduce miR156f expression (Supplementary Fig. S4A, B).

The involvement of auxin in MIM156fOE plants might favor the grain-filling process in dense-panicle plants

There is a great challenge to improve crop plant yield to provide enough food for the increasing world population. In a previous study, we isolated a dense-panicle T-DNA insertion mutant, A989, in which the *RCN2* gene was up-regulated (Nakagawa *et al.*, 2002; Li *et al.*, 2010). The seed setting per panicle in this mutant is approximately double that of the WT; however, approximately half of the seeds are empty. Therefore, the enhanced seed set in A989 is offset by the high ratio of vacant seeds (Fig. 8A). To improve the rice yield, the filling efficiency in the A989 mutant would need to be improved.

Because auxin signaling participates in the grain-filling process in rice (Liu *et al.*, 2015), we investigated whether the miR156–*OsSPL7*–*OsGH3.8* pathway might influence grain filling. To this end, we crossed the MIM156fOE plants with the A989 mutant. The hybrid had a similar number of tillers to that of the MIM156fOE plants, but the panicle was shortened and the seeds were densely set (Fig. 8A–C). However, the hybrid panicle had similar numbers of first and secondary branches as that of the A989 mutant (Fig. 8D). More importantly, the seed-filling efficiency of the hybrid was dramatically improved

(Fig. 8E). These results show that the MIM156fOE genetic background improves the grain-filling limitation of A989.

Discussion

It has been extensively reported that the function of miR156 is far ranging and conserved among different species (Huijser and Schmid, 2011; Wang and Wang, 2015). In this study, we showed that miR156f is a positive regulator of tiller number and a negative regulator of plant height. Consistent with its conserved function, several of the 12 *miR156* genes in rice have been reported as influencing tiller number and plant height (Xie *et al.*, 2006; Chen *et al.*, 2015; Hayashi-Tsugane *et al.*, 2015; Wang *et al.*, 2015). There are also 18 miR156 target *SPL* genes in rice, and the functions of some of these have already been determined (Jiao *et al.*, 2010; Miura *et al.*, 2010; Springer, 2010). We found that *SPL7*OE plants had a single tiller phenotype that has not previously been reported for other *SPL* genes (Fig. 3C). We also found that *SPL7*RNAi plants had a cluster and dwarf phenotype (Fig. 3E, F). Based on the concept that miRNAs negatively regulate expression of their targets, we determined that *OsSPL7* is a negative regulator of tiller number and *OsSPL7* functions as a downstream target of miR156f in regulating plant architecture (Vaucheret, 2006; Liu, 2008). At the same time, *OsSPL2* functions as a positive regulator of tiller number and a negative regulator of plant height, as confirmed by the cluster and dwarf phenotype of *OsSPL2*OE and *OsSPL2*GFP plants (Fig. 3E, F; Supplementary Fig. S5A). Therefore, it appears that the targets of miR156 might

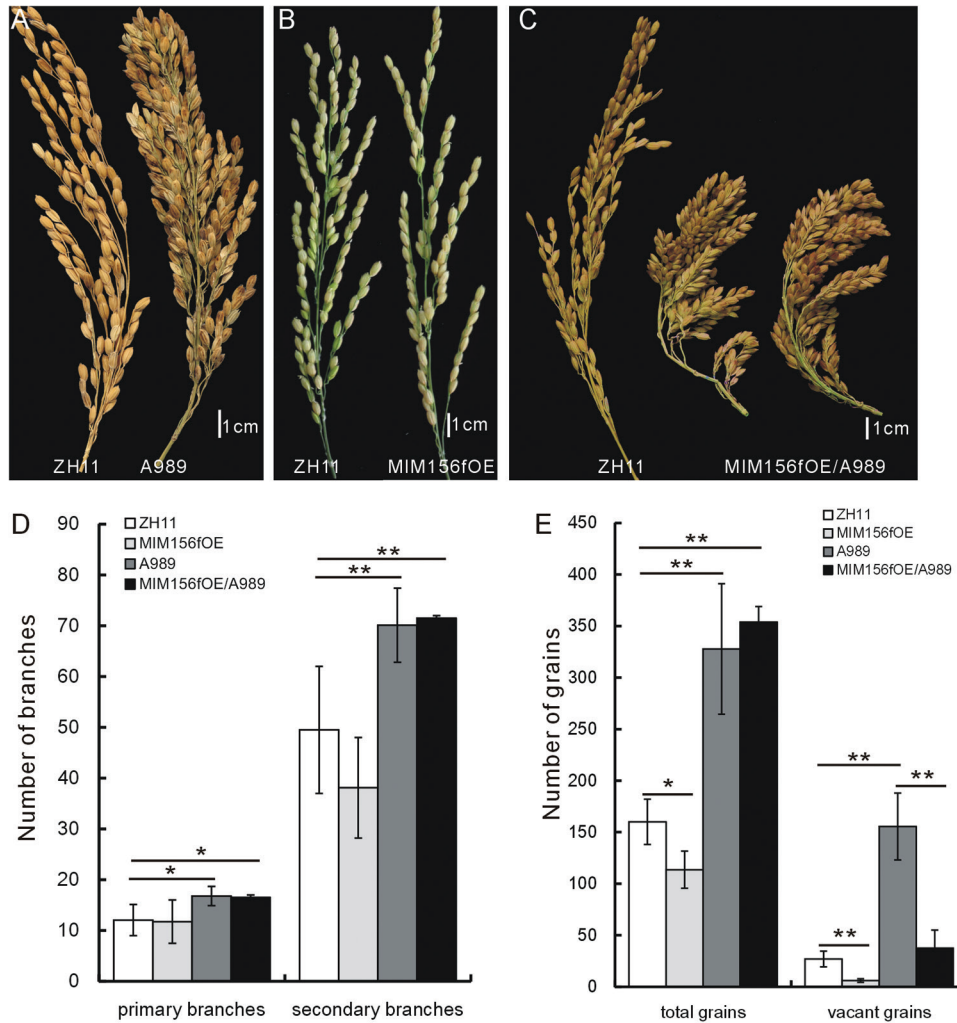


Fig. 8. MIM156fOE favored the grain-filling process in dense-panicle plants. (A–C) Panicles of A989 (A), MIM156fOE (B), and MIM156fOE/A989 (C) plants (the WT is shown to the left in each image for comparison). (D) Numbers of primary and secondary branches in the MIM156f/A989 hybrid, its parent lines, and the WT ($n=10$). (E) Numbers of total and vacant grains in the MIM156fOE/A989 hybrid, its parent lines, and the WT ($n=20$). The asterisks in (D) and (E) represent a significant difference, as determined by a Student's t -test at $*P<0.05$ and $**P<0.01$, respectively. (This figure is available in color at *JXB* online.)

function in the same processes, but the direction of regulation might differ. This might be a buffering mechanism to offset the cumulative effects of there being several targets of miR156. Supporting this hypothesis, we found that SPL7OE plants had a single tiller and were infertile (Fig. 3C), which is a phenotype that is more severe than that of the MIM156fOE plants (Fig. 2A).

In this study, we showed that there was direct binding of OsSPL7 to the OsGH3.8 promoter. From these data, together with genetic analysis of the interaction between miR156f and OsGH3.8, we demonstrated that the miR156f–OsSPL7–OsGH3.8 pathway is important in regulating rice plant architecture (Fig. 7). We also found that miR156f overexpression caused a cluster and dwarf phenotype (Fig. 1), the development of ectopic shoots, and disturbed axillary bud dormancy (Supplementary Fig. S2D). These features are associated with alterations in auxin signaling. However, our analysis did not rule out the possible involvement of other targets (such as OsSPL2) and additional factors that could regulate plant

architecture. Based on the following observations, we propose that there might also be additional pathways through which miR156f is involved in auxin signaling in addition to the miR156f–OsSPL7–OsGH3.8 pathway. First, the tiller number and plant height of the *cd* mutant were partially complemented by OsGH3.8R plants (Fig. 6D, E). Secondly, although the SPL7RNAi and GH3.8OE plants both had increased numbers of tillers and reduced plant heights, neither of these plant lines had phenotypes that were as pronounced as those in the *cd* mutant (Figs 3E, F, 6B; Supplementary Fig. S5B).

In this study, the OsSPL7 activity had obvious dosage effects. These were associated not only with the tiller number but also with fertility, with high OsSPL7 expression in SPL7OE plants resulting in infertility (Fig. 3C, D). In the SPL7Flag plants and the MIM156fOE plants where the OsSPL7 levels were not as highly up-regulated (Fig. 3D; Supplementary Fig. S1B), the grain-filling efficiency and fertility were restored. Furthermore, the low grain-filling efficiency of the A989 mutant was greatly enhanced by hybridization with the MIM156fOE plant line.

Therefore, both miR156f and *OsSPL7* might have roles in regulating fertility. This hypothesis is supported by previous discussions of the possible roles of the miR156/SPL in fertility regulation in Arabidopsis (Huijser and Schmid, 2011) and rice (Wang and Wang, 2015), and further extends the possible roles of miR156. Auxin is also a multifunctional factor in plant development. The combined actions of miR156 and auxin might also mediate changes in fertility such as that demonstrated by the crossing of MIM156fOE and A989 (Fig. 8). Therefore, crosstalk between important developmental and physiological factors such as miR156f and auxin might be important for modulating plant development and physiology in more than one aspect of plant growth.

Supplementary data

Supplementary data are available at *JXB* online.

Table S1. Primer sequences used in this study.

Table S2. Co-segregation analysis of the T-DNA insert and the cluster and dwarf phenotype in the F₂ population obtained from the reciprocal cross and backcross between WT and the *cd* mutant.

Table S3. Microarray analysis of the *cd* mutant as compared with the WT.

Fig S1. Gene expression in the miR156f-related plant lines.

Fig S2. Further phenotypes of MIM156fOE and the *cd* mutant.

Fig S3. *OsGH3.8* expression in miR156f/*OsSPL7*-related genetic lines and confirmation of the cross between the GH3.8OE and MIM156fOE plants.

Fig S4. miR156f and *OsGH3.8* expression in response to NAA treatment.

Fig S5. qRT-PCR analysis of *OsSPL2* expression in the *OsSPL2*OE and *OsSPL2*GFP plants (A) and statistical analysis of the plant height and tiller number in the *cd* mutant, *SPL7*RNAi and GH3.8OE plants (B).

Acknowledgements

We would like to thank Jiawei Wang from our institute for helpful suggestions on this work. This work was supported by the National Key R&D Program of China (2016YFD0100600), the National Special Program on Research and Commercialization of Transgenic Plant (2016ZX08009-003-001, 2014ZX08009-003-003), Scholarship Foundation from Shanghai Institutes for Biological Sciences (2007KIP206), and the SA-SIBS 2009 Young Faculty Award. We thank Shelley Robison, PhD, from Liwen Bianji, Edanz Group China (www.liwenbianji.cn/ac, accessed 27 July 2018), for editing the English text of a draft of this manuscript. The authors declare no conflict of interest.

References

Aravin AA, Lagos-Quintana M, Yalcin A, Zavolan M, Marks D, Snyder B, Gaasterland T, Meyer J, Tuschl T. 2003. The small RNA profile during *Drosophila melanogaster* development. *Developmental Cell* **5**, 337–350.

Bartel B, Bartel DP. 2003. MicroRNAs: at the root of plant development? *Plant Physiology* **132**, 709–717.

Bartel DP. 2004. MicroRNAs: genomics, biogenesis, mechanism, and function. *Cell* **116**, 281–297.

Bartel DP. 2009. MicroRNAs: target recognition and regulatory functions. *Cell* **136**, 215–233.

Bergonzi S, Albani MC, Ver Loren van Themaat E, Nordström KJ, Wang R, Schneeberger K, Moerland PD, Coupland G. 2013. Mechanisms of age-dependent response to winter temperature in perennial flowering of *Arabis alpina*. *Science* **340**, 1094–1097.

Bhogale S, Mahajan AS, Natarajan B, Rajabhoj M, Thulasiram HV, Banerjee AK. 2014. MicroRNA156: a potential graft-transmissible microRNA that modulates plant architecture and tuberization in *Solanum tuberosum* ssp. *andigena*. *Plant Physiology* **164**, 1011–1027.

Chen Q, Westfall CS, Hicks LM, Wang S, Jez JM. 2010. Kinetic basis for the conjugation of auxin by a GH3 family indole-acetic acid-amido synthetase. *Journal of Biological Chemistry* **285**, 29780–29786.

Chen Z, Gao X, Zhang J. 2015. Alteration of osa-miR156e expression affects rice plant architecture and strigolactones (SLs) pathway. *Plant Cell Reports* **34**, 767–781.

Cho SH, Coruh C, Axtell MJ. 2012. miR156 and miR390 regulate tasiRNA accumulation and developmental timing in *Physcomitrella patens*. *The Plant Cell* **24**, 4837–4849.

Cui LG, Shan JX, Shi M, Gao JP, Lin HX. 2014. The miR156–SPL9–DFR pathway coordinates the relationship between development and abiotic stress tolerance in plants. *The Plant Journal* **80**, 1108–1117.

Dai Z, Wang J, Zhu M, Miao X, Shi Z. 2016. OsMADS1 represses microRNA172 in elongation of palea/lemma development in rice. *Frontiers in Plant Science* **7**, 1891.

Ferreira e Silva GF, Silva EM, Azevedo Mda S, Guivin MA, Ramiro DA, Figueiredo CR, Carrer H, Peres LE, Nogueira FT. 2014. microRNA156-targeted SPL/SBP box transcription factors regulate tomato ovary and fruit development. *The Plant Journal* **78**, 604–618.

Franco-Zorrilla JM, Valli A, Todesco M, et al. 2007. Target mimicry provides a new mechanism for regulation of microRNA activity. *Nature Genetics* **39**, 1033–1037.

Gou JY, Felippes FF, Liu CJ, Weigel D, Wang JW. 2011. Negative regulation of anthocyanin biosynthesis in Arabidopsis by a miR156-targeted SPL transcription factor. *The Plant Cell* **23**, 1512–1522.

Hayashi-Tsugane M, Maekawa M, Tsugane K. 2015. A gain-of-function Bushy dwarf tiller 1 mutation in rice microRNA gene miR156d caused by insertion of the DNA transposon nDart1. *Scientific Reports* **5**, 14357.

Hellens RP, Allan AC, Friel EN, Bolitho K, Grafton K, Templeton MD, Karunairetnam S, Gleave AP, Laing WA. 2005. Transient expression vectors for functional genomics, quantification of promoter activity and RNA silencing in plants. *Plant Methods* **1**, 13.

Hiei Y, Ohta S, Komari T, Kumashiro T. 1994. Efficient transformation of rice (*Oryza sativa* L.) mediated by Agrobacterium and sequence analysis of the boundaries of the T-DNA. *The Plant Journal* **6**, 271–282.

Higuchi R, Krummel B, Saiki RK. 1988. A general method of in vitro preparation and specific mutagenesis of DNA fragments: study of protein and DNA interactions. *Nucleic Acids Research* **16**, 7351–7367.

Huijser P, Schmid M. 2011. The control of developmental phase transitions in plants. *Development* **138**, 4117–4129.

Jain M, Khurana JP. 2009. Transcript profiling reveals diverse roles of auxin-responsive genes during reproductive development and abiotic stress in rice. *FEBS Journal* **276**, 3148–3162.

Jia X, Mendu V, Tang G. 2010. An array platform for identification of stress-responsive microRNAs in plants. *Methods in Molecular Biology* **639**, 253–269.

Jiao Y, Wang Y, Xue D, et al. 2010. Regulation of OsSPL14 by OsmiR156 defines ideal plant architecture in rice. *Nature Genetics* **42**, 541–544.

Jones-Rhoades MW. 2012. Conservation and divergence in plant microRNAs. *Plant Molecular Biology* **80**, 3–16.

Jones-Rhoades MW, Bartel DP, Bartel B. 2006. MicroRNAs and their regulatory roles in plants. *Annual Review of Plant Biology* **57**, 19–53.

LeClere S, Tellez R, Rampey RA, Matsuda SP, Bartel B. 2002. Characterization of a family of IAA-amino acid conjugate hydrolases from Arabidopsis. *Journal of Biological Chemistry* **277**, 20446–20452.

Li L, Shi Z, Shen G, Wang X, An L, Zhang L. 2010. Dense-panicle-related gene cloning from rice mutant A989 and transgenic plant analysis (in Chinese). *Acta Agronomica Sinica* **36**, 887–894.

Li X, Qian Q, Fu Z, et al. 2003. Control of tillering in rice. *Nature* **422**, 618–621.

Liu J. 2008. Control of protein synthesis and mRNA degradation by microRNAs. *Current Opinion in Cell Biology* **20**, 214–221.

- Liu L, Tong H, Xiao Y, Che R, Xu F, Hu B, Liang C, Chu J, Li J, Chu C. 2015. Activation of Big Grain1 significantly improves grain size by regulating auxin transport in rice. *Proceedings of the National Academy of Sciences, USA* **112**, 11102–11107.
- Liu YG, Mitsukawa N, Oosumi T, Whittier RF. 1995. Efficient isolation and mapping of *Arabidopsis thaliana* T-DNA insert junctions by thermal asymmetric interlaced PCR. *The Plant Journal* **8**, 457–463.
- Ljung K, Hull AK, Kowalczyk M, Marchant A, Celenza J, Cohen JD, Sandberg G. 2002. Biosynthesis, conjugation, catabolism and homeostasis of indole-3-acetic acid in *Arabidopsis thaliana*. *Plant Molecular Biology* **49**, 249–272.
- Miura K, Ikeda M, Matsubara A, Song XJ, Ito M, Asano K, Matsuoka M, Kitano H, Ashikari M. 2010. OsSPL14 promotes panicle branching and higher grain productivity in rice. *Nature Genetics* **42**, 545–549.
- Nakagawa M, Shimamoto K, Kyojuka J. 2002. Overexpression of RCN1 and RCN2, rice TERMINAL FLOWER 1/CENTRORADIALIS homologs, confers delay of phase transition and altered panicle morphology in rice. *The Plant Journal* **29**, 743–750.
- Nelson P, Kiriakidou M, Sharma A, Maniataki E, Mourelatos Z. 2003. The microRNA world: small is mighty. *Trends in Biochemical Sciences* **28**, 534–540.
- Nischal L, Mohsin M, Khan I, Kardam H, Wadhwa A, Abrol YP, Iqbal M, Ahmad A. 2012. Identification and comparative analysis of microRNAs associated with low-N tolerance in rice genotypes. *PLoS One* **7**, e50261.
- Nodine MD, Bartel DP. 2010. MicroRNAs prevent precocious gene expression and enable pattern formation during plant embryogenesis. *Genes & Development* **24**, 2678–2692.
- Rampey RA, LeClere S, Kowalczyk M, Ljung K, Sandberg G, Bartel B. 2004. A family of auxin-conjugate hydrolases that contributes to free indole-3-acetic acid levels during *Arabidopsis* germination. *Plant Physiology* **135**, 978–988.
- Rhoades MW, Reinhart BJ, Lim LP, Burge CB, Bartel B, Bartel DP. 2002. Prediction of plant microRNA targets. *Cell* **110**, 513–520.
- Sauer M, Robert S, Kleine-Vehn J. 2013. Auxin: simply complicated. *Journal of Experimental Botany* **64**, 2565–2577.
- Song A, Wang L, Chen S, Jiang J, Guan Z, Li P, Chen F. 2015. Identification of nitrogen starvation-responsive microRNAs in *Chrysanthemum nankingense*. *Plant Physiology and Biochemistry* **91**, 41–48.
- Springer N. 2010. Shaping a better rice plant. *Nature Genetics* **42**, 475–476.
- Staswick PE, Tiryaki I, Rowe ML. 2002. Jasmonate response locus JAR1 and several related *Arabidopsis* genes encode enzymes of the firefly luciferase superfamily that show activity on jasmonic, salicylic, and indole-3-acetic acids in an assay for adenylation. *The Plant Cell* **14**, 1405–1415.
- Stief A, Altmann S, Hoffmann K, Pant BD, Scheible WR, Bäurle I. 2014. *Arabidopsis* miR156 regulates tolerance to recurring environmental stress through SPL transcription factors. *The Plant Cell* **26**, 1792–1807.
- Terol J, Domingo C, Talón M. 2006. The GH3 family in plants: genome wide analysis in rice and evolutionary history based on EST analysis. *Gene* **371**, 279–290.
- Vaucheret H. 2006. Post-transcriptional small RNA pathways in plants: mechanisms and regulations. *Genes & Development* **20**, 759–771.
- Wang H, Wang H. 2015. The miR156/SPL module, a regulatory hub and versatile toolbox, gears up crops for enhanced agronomic traits. *Molecular Plant* **8**, 677–688.
- Wang J, Gao X, Li L, Shi X, Zhang J, Shi Z. 2010. Overexpression of *Osta-siR2141* caused abnormal polarity establishment and retarded growth in rice. *Journal of Experimental Botany* **61**, 1885–1895.
- Wang J, Li L, Wan X, An L, Zhang J. 2004. Distribution of T-DNA carrying a Ds element on rice chromosomes. *Science in China. Series C, Life Sciences* **47**, 322–331.
- Wang JW. 2014. Regulation of flowering time by the miR156-mediated age pathway. *Journal of Experimental Botany* **65**, 4723–4730.
- Wang L, Sun S, Jin J, *et al.* 2015. Coordinated regulation of vegetative and reproductive branching in rice. *Proceedings of the National Academy of Sciences, USA* **112**, 15504–15509.
- Wang M, Wang Q, Zhang B. 2013. Response of miRNAs and their targets to salt and drought stresses in cotton (*Gossypium hirsutum* L.). *Gene* **530**, 26–32.
- Wang S, Wu K, Yuan Q, *et al.* 2012. Control of grain size, shape and quality by OsSPL16 in rice. *Nature Genetics* **44**, 950–954.
- Westfall CS, Herrmann J, Chen Q, Wang S, Jez JM. 2010. Modulating plant hormones by enzyme action: the GH3 family of acyl acid amido synthetases. *Plant Signaling & Behavior* **5**, 1607–1612.
- Woodward AW, Bartel B. 2005. Auxin: regulation, action, and interaction. *Annals of Botany* **95**, 707–735.
- Wu G, Park MY, Conway SR, Wang JW, Weigel D, Poethig RS. 2009. The sequential action of miR156 and miR172 regulates developmental timing in *Arabidopsis*. *Cell* **138**, 750–759.
- Xie K, Shen J, Hou X, Yao J, Li X, Xiao J, Xiong L. 2012. Gradual increase of miR156 regulates temporal expression changes of numerous genes during leaf development in rice. *Plant Physiology* **158**, 1382–1394.
- Xie K, Wu C, Xiong L. 2006. Genomic organization, differential expression, and interaction of SQUAMOSA promoter-binding-like transcription factors and microRNA156 in rice. *Plant Physiology* **142**, 280–293.
- Xing S, Salinas M, Garcia-Molina A, Höhmann S, Berndtgen R, Huijser P. 2013. SPL8 and miR156-targeted SPL genes redundantly regulate *Arabidopsis* gynoecium differential patterning. *The Plant Journal* **75**, 566–577.
- Xue XY, Zhao B, Chao LM, Chen DY, Cui WR, Mao YB, Wang LJ, Chen XY. 2014. Interaction between two timing microRNAs controls trichome distribution in *Arabidopsis*. *PLoS Genetics* **10**, e1004266.
- Yoshida A, Ohmori Y, Kitano H, Taguchi-Shiobara F, Hirano HY. 2012. Aberrant spikelet and panicle1, encoding a TOPLESS-related transcriptional co-repressor, is involved in the regulation of meristem fate in rice. *The Plant Journal* **70**, 327–339.
- Yu N, Niu QW, Ng KH, Chua NH. 2015. The role of miR156/SPLs modules in *Arabidopsis* lateral root development. *The Plant Journal* **83**, 673–685.
- Yu S, Galvão VC, Zhang YC, *et al.* 2012. Gibberellin regulates the *Arabidopsis* floral transition through miR156-targeted SQUAMOSA promoter binding-like transcription factors. *The Plant Cell* **24**, 3320–3332.
- Yu S, Lian H, Wang JW. 2015. Plant developmental transitions: the role of microRNAs and sugars. *Current Opinion in Plant Biology* **27**, 1–7.
- Yu ZX, Wang LJ, Zhao B, Shan CM, Zhang YH, Chen DF, Chen XY. 2015. Progressive regulation of sesquiterpene biosynthesis in *Arabidopsis* and Patchouli (*Pogostemon cablin*) by the miR156-targeted SPL transcription factors. *Molecular Plant* **8**, 98–110.
- Zhang Q. 2007. Strategies for developing Green Super Rice. *Proceedings of the National Academy of Sciences, USA* **104**, 16402–16409.
- Zhao SQ, Xiang JJ, Xue HW. 2013. Studies on the rice LEAF INCLINATION1 (LC1), an IAA-amido synthetase, reveal the effects of auxin in leaf inclination control. *Molecular Plant* **6**, 174–187.
- Zhou L, Liu Y, Liu Z, Kong D, Duan M, Luo L. 2010. Genome-wide identification and analysis of drought-responsive microRNAs in *Oryza sativa*. *Journal of Experimental Botany* **61**, 4157–4168.